Polymer-Induced Transient Networks in Water-in-Oil Microemulsions Studied by Small-Angle X-Ray and Dynamic Light Scattering

T. Blochowicz,* C. Gögelein, T. Spehr, M. Müller, and B. Stühn
TU-Darmstadt, 64289 Darmstadt, Germany

We study water-in-oil microemulsions, in particular dispersions of water droplets coated with a monolayer of the anionic surfactant AOT in a continuous phase of n-decane. Upon addition of the amphiphilic triblock copolymer PEO(polyethylenoxide)-PI(polyisoprene)-PEO a transient network is formed. At constant droplet size we vary the polymer concentration and there is clear evidence for an increasing crosslinking of the droplets from structural investigations with small-angle X-ray scattering (SAXS). The dynamics of concentration fluctuations consisting of the translational diffusion of the droplets and the relaxation of the network are monitored with photon correlation spectroscopy (PCS). We mainly focus on the variation of the dynamic behaviour as a function of the number of polymer molecules per droplet and the droplet volume fraction, which may be taken as a measure for the inter-droplet distance. With increasing polymer content the dynamics of the system slows down and three different relaxation processes may be distinguished. We discuss the origin of the different relaxation modes. In particular it turns out that the intermediate relaxation mode may be suppressed by index matching the oil matrix and the PI block and that it is effectively slowed down by an additional loading of the emulsion droplets with polyethylene glycol of increasing molecular weight.

I. INTRODUCTION

The idea of a transient network, i.e. the temporary existence of crosslinks, which lead to an elastic response of the material at short times, whereas viscous flow takes over at longer timescales, has long been known as one of the ways to exemplify and understand relaxation behaviour in viscoelastic materials [1]. On the other hand understanding network formation and the related structural and dynamical properties in itself comprises an active field of current research (cf. *e. g.* [2, 3]) with a wide range of applications in science and industry.

In the present work we are interested in a particularly suitable model system, the solution of an amphiphilic triblock copolymer in the L_2 droplet phase of a water-in-oil microemulsion. The microemulsion consists of nanometer-size water droplets in an oil (decane) matrix stabilised by the anionic surfactant AOT (sodium bis(2-ethylhexyl)sulfosuccinate). Structure and phase behaviour of such microemulsions are well investigated [4] and the systems, though being complex on a molecular level, are considered as simple model systems in terms of a liquid of droplets on a nanometer scale, where mostly droplet-droplet interaction can be described in terms of simple hard-sphere potentials [4]. As an amphiphilic triblock copolymer we use polyethylene oxide(PEO) - polyisoprene(PI) - PEO so that its ends are selectively soluble in the droplet water cores, whereas the middleblock only dissolves in the oily environment. Thus, upon addition of polymer either decoration of single droplets (loops) or bridging into a transient network (arcs) may occur, cf. Fig. 1. In the latter configuration the system has the convenient advantage over comparable network forming

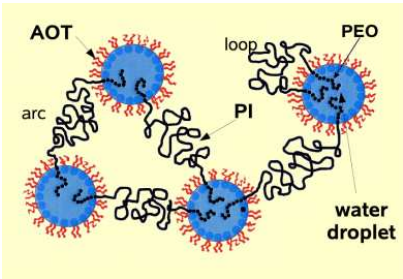

FIG. 1: (Color online) Schematic representation of the water-in oil microemulsion with triblock copolymer PEO-PI-PEO both in decoration and bridging configuration.

systems, like semi-dilute polymer solutions, that the volume density of network junction points (droplets) ϕ and the concentration of polymer chains per droplet Z may be varied independently in order to systematically distinguish their influence on network formation.

Whether the triblock copolymer just decorates single droplets or forms bridges in between droplets, in both cases the interdroplet interaction potential will effectively be changed by the polymer chains. Thus, one of the questions to be addressed in the following is how polymer concentration affects the droplet-droplet interactions and the overall structure of the system. We will focus on this question in the context of small angle X-ray scattering experiments which give structural information on the nanometer scale. Dynamics, on the other hand, will be probed by photon correlation spectroscopy (PCS), which is a powerful tool to investigate the relaxation dynamics in colloidal systems as well as polymer solutions and melts [5, 6]. In particular, as the problems encountered when investigating non-ergodic samples like in polymer gels [7, 8] are absent in our case due to the transient nature of the network, the method may be applied in a

*e-mail: thomas.blochowicz@physik.tu-darmstadt.de

most straightforward manner.

Pioneering experiments on the dynamics of a network forming system similar to ours (PEO-PI-PEO in water-AOT-isooctane) were done by Eicke and coworkers in the 90ies mostly by applying rheological measurements and dynamic light scattering [9–11], but also pulsed field gradient NMR [12, 13], transient optical birefringence [14] and conductivity measurements [15]. Later on Bagger-Jörgensen *et al.* initiated a series of experiments on oil-in-water microemulsions with the non-ionic surfactant $C_{12}E_5$ [16] and also in more recent publications direct [17–22] as well as inverse microemulsions [23, 24] are studied and either triblock copolymers or appropriately end-capped hydrophobic or hydrophilic polymers are used to induce network formation.

In many cases dynamics was studied by PCS and, depending on the particular system, two or three relaxation modes are reported, the origin of which is still a matter of debate: Whereas the fastest mode, which is found to be diffusive throughout, is usually ascribed to collective droplet diffusion or an overdamped gel mode at high polymer concentration [12, 16, 17, 20], for the intermediate and the slowest mode the situation is more difficult: In some cases only two modes are observed altogether, the fast being diffusive and the slow mode being independent of the scattering vector q [18], in other instances both modes are dominated by diffusion [25], depending on whether an inverse system or a direct o/w microemulsion is considered. In other inverse w/o microemulsions three diffusive modes were found [10, 12, 13] whereas more recent investigations on direct systems report an intermediate mode, which is q independent, in between two diffusive modes [17, 20, 21]. In the latter case it was shown by fluorescence recovery after photobleaching (FRAP) that the slowest diffusive mode was related to long-distance self diffusion of the nanodroplets [20] whereas comparison of the intermediate relaxation time with the terminal relaxation time of an oscillatory shear experiment indicated that the intermediate mode is connected with the lifetime of the network junctions [17].

In order to understand the q dependence of the two fast relaxation modes, recently the Brochard-de Gennes two-fluids model for semi-dilute polymer solutions was generalised and successfully applied to polymer induced transient networks in direct microemulsions by Michel *et al.* [21]. In particular it was shown that depending on the collective and the viscoelastic diffusion constant and the terminal relaxation time either one diffusive and one q independent mode should be observed or in both modes a crossover from q independence to a q^2 behaviour of the inverse relaxation times is expected. For systems based on direct microemulsions good agreement between data and model is reported [21], however, previous studies based on inverse microemulsion systems, which report two, respectively, three diffusive processes [10, 12, 13, 25], seem to show different behaviour. In the present contribution we will focus on such a system also with the aim to allow for a systematic comparison of transient polymer induced networks formed in direct and inverse microemulsions. Thus, we will investigate structure and dynamics of the system upon an independent variation of droplet volume fraction and polymer concentration. Additional experiments like index matching of the midblock and an extra loading of the micelles with a suitable polymer will help in interpreting the dynamic modes observed in the light scattering experiment.

II. EXPERIMENTAL

A. Materials and Sample Preparation

The microemulsions were prepared using deionized water from a Millipore Direct-Q 3 ultrapure water system and decane of 99%+ purity from Acros Organics without further treatment. The surfactant AOT (sodium bis[2-ethylhexyl] sulfosuccinate, quality grade microselect) was purchased from Fluka and used as received. AOT was stored under dry Argon atmosphere and a stock solution of AOT in decane was prepared in a glove box in order to avoid an uncontrolled water absorption due to the surfactant being hygroscopic. Finally the microemulsions were prepared by adding appropriate amounts of water and decane. Thus, the composition of each system is determined by two parameters, the molar ratio ω of water to surfactant molecules:

$$\omega = \frac{[H_2O]}{[AOT]},$$

which was kept fixed at $\omega = 40$ for all systems studied, and the droplet volume fraction ϕ:

$$\phi = \frac{V_w + V_{AOT}}{V_w + V_{AOT} + V_d},$$

which varies by the respective volume of the components water (w) decane (d) and AOT. At all temperatures and compositions investigated in this work the microemulsion system is located in the L_2 non-conducting droplet region of the phase diagram [4, 26].

The triblock copolymer PEO-PI-PEO was purchased from Polymer Standards Service (Mainz, Germany) with the molecular weight of the PEO end blocks being $m_{PEO} = 12300\,\mathrm{g/mol}$ and that of the PI mid block being $m_{PI} = 43400\,\mathrm{g/mol}$. From the same manufacturer we purchased pure PI identical to the midblock of the copolymer and determined the average end-to-end distance by dissolving PI in decane at various concentrations. We determined the hydrodynamic radius by PCS as $R_H = 11.1 \pm 0.2\,\mathrm{nm}$ and so the end-to-end distance yields $R_{EE} = 27.2 \pm 0.6\,\mathrm{nm}$. At an interdroplet spacing of this order or below we expect formation of transient polymer networks. Note that it was not possible to dissolve significant amounts of the triblock copolymer either in pure decane or in pure water. Thus we do not expect the polymer to form micelles of its own.

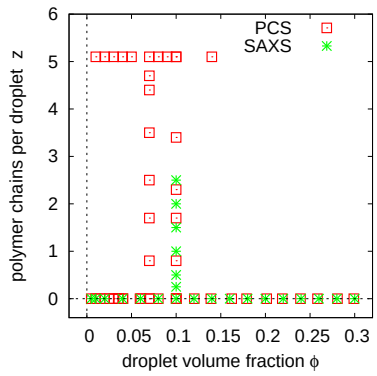

FIG. 2: (Color online) Polymer concentration versus droplet volume fraction of the systems investigated in the present work. The applied methods are photon correlation spectroscopy and small angle X-ray scattering as indicated.

The content of triblock copolymer, which is added to each microemulsion, is determined by the number Z of polymer chains per droplet, the number of droplets in a certain volume being given by the ratio $3V_{\rm w}/4\pi R_{\rm w}^3$, where $R_{\rm w}$ is the water core radius as determined by SAXS. After addition of polymer the mixture was stirred for several days at $T \approx 60\,^{\circ}$C to ensure homogeneous mixing. After the stirring the samples were kept at room temperature for again a few days before being measured. We note here that in contrast to a previous report by Batra *et al.* [27] but in accordance with observations in similar systems by Eicke and coworkers [9–14, 25] we do not observe any phase separation in our samples. As it is shown in Fig. 2 we cover a range in droplet volume fraction of $\phi = 0.01 \ldots 0.14$ at a polymer content of $Z = 5.1$ and in particular at low ϕ and $Z = 5.1$ even after storing the samples for more than six months under ambient conditions no phase separation is observed.

B. Small Angle X-Ray Scattering

In order to characterise the structure of the pure as well as the polymer containing microemulsions we applied small angle X-ray scattering. The X-ray beam is produced by an Analytical PW-2273 X-ray tube. The beam passes through a Ni-filter to yield CuK$_\alpha$ radiation at $\lambda = 1.54\,$Å, which then is point-collimated by three pinholes. The scattered intensity is recorded with a 2-dimensional multiwire detector by Molecular Metrology at a distance of 150 cm from the sample leading to an accessible range of scattering vectors $q = 0.008\,\text{Å}^{-1} \ldots 0.25\,\text{Å}^{-1}$. The samples were filled into borosilicate glass capillaries of 2 mm in diameter and inserted into a Linkam temperature controller stage mounted in the sample chamber. All SAXS experiments were performed at a temperature of $T = 288\,$K with the temperature being controlled with an accuracy of $\pm 0.1\,$K.

C. Photon Correlation Spectroscopy

The quasielastic light scattering experiments were performed on a standard goniometer (ALV) at scattering angles between 30° and 150° using a HeNe Laser with a wavelength of $\lambda = 632.5\,$nm with a vertically polarised incident beam and a vertical polarisation filter in front of the detection unit (VV geometry). The sample cuvette was thermostated in a cylindrical vat filled with ethanol to meet index matching conditions. Temperature was regulated with an absolute accuracy of $\pm 0.5\,$K. The normalised autocorrelation function of the scattered light intensity $g_2(t)$ was recorded by using a ALV-5000/E hardware correlator card and in Gaussian approximation the correlation function $g_1(t)$ of the electric field was calculated as $g_1^2(t) = (g_2(t) - 1)/f_A$ with $0 < f_A < 1$ being the coherence factor due to the integrating effect of a finite detector area.

III. THE STRUCTURE MODEL

In order to extract the structural information from the X-ray data, the following model will be employed. The intensity $I(q)$ of scattered X-rays in the SAXS experiment for an isotropic system of identical particles can be described in terms of a single particle form factor $F(q)$ and an interference function or structure factor $S(q)$:

$$I(q) = C\,F^2(q)\;S(q) + I_b \tag{1}$$

with I_b denoting the scattering background due to density fluctuations and C being a prefactor, which contains the number density of scattering particles. For the general case of n shells around a spherical droplet core the form factor reads:

$$F_n(q) = 4\pi \sum_{i=0}^{n} \Delta\rho_i \left(\frac{\sin(qR_i) - qR_i\cos(qR_i)}{q^3} \right), \tag{2}$$

where R_i is the radius of the ith shell or, respectively, the core R_0 and $\Delta\rho_i = \rho_i - \rho_{i+1}$ is the electron density contrast between the shells i and $i+1$ with ρ_{n+1} and ρ_0 being the electron density of the solvent and the core, respectively. So, for a simple core-shell micelle $n = 1$ and $F_1(q)$ contains two terms, one from the scattering of the core the other from scattering of the shell. For a homogeneous and isotropic system the structure factor is given by the Fourier transform of the pair correlation function $h(r)$ as follows:

$$S(q) = 1 + 4\pi\, n \int_0^\infty h(r)\, \frac{\sin(qr)}{qr}\, r^2\, \mathrm{d}r \tag{3}$$

with n being the particle number density.

In the case of polydisperse scatterers it can be shown [28, 29] that if the polydispersity of the particles and their relative distances are uncorrelated then again a simple

expression for the scattered intensity can be obtained by applying appropriate averages in Eq. (1):

$$I(q) = C\ \left(\langle|F(q)|\rangle^2 S(q) + \langle|F(q)|^2\rangle - \langle|F(q)|\rangle^2\right) + I_b, \tag{4}$$

where $\langle\ldots\rangle$ denotes an average over a distribution of radii, *i. e.* we only consider size polydispersity, as size and shape polydispersity cannot be distinguished in the SAXS experiment. To calculate the averages we choose a gamma distribution as the distribution of radii:

$$f(R, \bar{R}, \sigma_R) = \left(\frac{R\bar{R}}{\sigma_R^2}\right)^{\bar{R}^2/\sigma_R^2} \frac{\exp(-R\bar{R}/\sigma_R^2)}{R\,\Gamma(\bar{R}^2/\sigma_R^2)} \tag{5}$$

with the average radius $\bar{R}$ and the root mean square deviation σ_R. Note that, as opposed to *e. g.* a Gaussian distribution of radii Eq. (5) has the advantage that the unphysical case of a finite contribution of negative radii is excluded.

In order to model the structure factor $S(q)$ we employ the Percus-Yevick closure for the direct correlation function $c(r)$ in the Ornstein Zernicke equation:

$$c(r) = \left(1 - e^{\Phi(r)/k_B T}\right)(h(r) + 1) \tag{6}$$

which contains the pair interaction potential $\Phi(r)$. As a first approximation we assume a hard sphere potential for $\Phi(r)$, for which the Ornstein-Zernicke equation with the above closure can be solved analytically [30, 31]. Thus, the expression for $S(q)$, which is not reproduced here in detail, contains a hard-sphere radius $R_{\rm HS}$ and the volume fraction of hard spheres $\eta_{\rm HS}$ as parameters. Finally, the q-dependent terms in eq. (4) are convoluted with the instrumental resolution function, which is obtained from the interference peaks in the intensity profile of silver behenate, and a constant background is added. Note that for all fit parameters to be shown in the following the standard error estimates of the fit procedure lie within the size of the symbols.

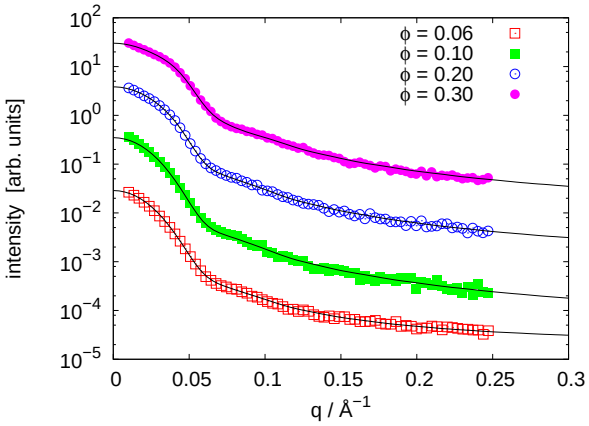

FIG. 3: (Color online) SAXS Intensity profile of the pure microemulsion system water-AOT-decane for a droplet size of $\omega = 40$ and selected droplet volume fractions ϕ. Each data set is vertically shifted by a factor of ten. The solid lines show fits of the hard-sphere model described by eq. (4).

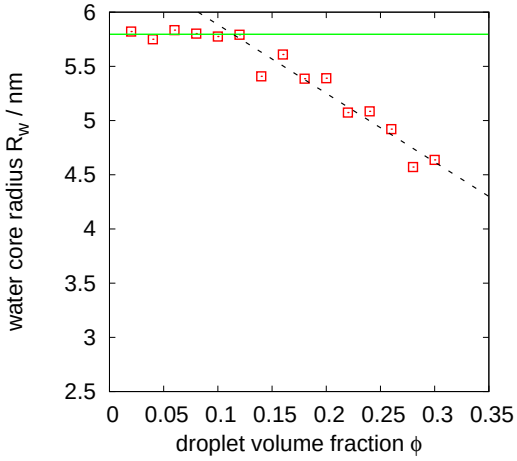

FIG. 4: (Color online) The water core radius $R_{\rm w}$ of the pure microemulsion as a function of droplet volume fraction. Up to $\phi \approx 0.12$ size and volume fraction (*i. e.* average distance of the droplets) are independent quantities.

IV. RESULTS AND DISCUSSION

A. Pure Microemulsions

In order to determine structural changes in the microemulsion system due to the formation of a transient network upon addition of polymer, we first characterised the microemulsions without polymer at $\omega = 40$ in a droplet volume fraction range of $0.01 \leq \phi \leq 0.3$ by SAXS and PCS at a temperature of $T = 288\,\mathrm{K}$.

The SAXS data are shown in Fig. 3. The solid lines represent fits with eq. (4), where a simple core-shell model for the form factor ($F_1(q)$ from eq. (2)) and the hard sphere interaction potential in eq. (6) were used. In that way an excellent description of the data is obtained in the full range of q. It turns out that the water core radius is proportional to ω, as expected. Ideally, this radius would be independent of the droplet volume fraction, however, it turns out that this holds only true for rather low ϕ. Fig. 4 shows the water core radius as a function of droplet volume fraction for $\omega = 40$. Upto a value of $\phi \approx 0.12$ a constant water core radius of $R_{\rm w} = 5.8\,\mathrm{nm}$ is observed, whereas above it decreases continuously. At the same time the radial polydispersity of about 27% and the shell thickness of $\delta \approx 2.8\,\mathrm{Å}$ remain constant within experimental accuracy for all droplet concentrations.

Note that, while it is widely assumed in the literature that in the present microemulsion system the droplet radius is completely determined by ω, Seto et al. have reported an observation similar to ours at large droplet volume fractions $0.4 \leq \phi \leq 0.6$ [32]. They suggested that

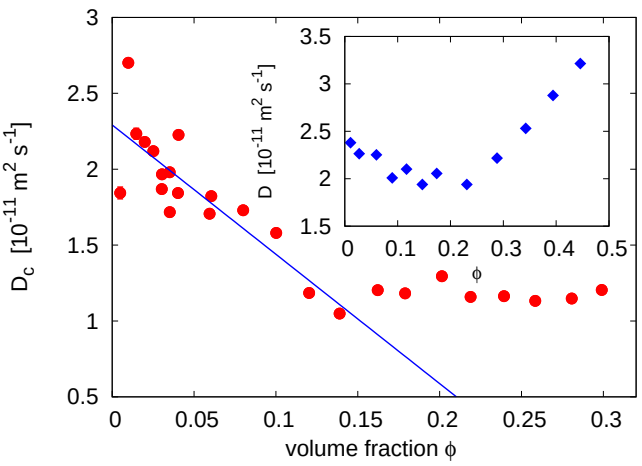

FIG. 5: (Color online) The collective diffusion coefficient D_c of the pure microemulsion system as a function of droplet volume fraction ϕ. Out of the linear range at low ϕ the free diffusion constant D_0 is determined. Inset: Comparable plot for an oil-in-water microemulsion with non-ionic surfactant $C_{12}E_5$ taken from [17].

the decrease in droplet radius is due to the shape of the micelles increasingly deviating from an ideal sphere in order to achieve higher packing densities at large droplet volume fractions. However, a quick calculation shows that the radius of gyration of an ellipsoid with ratio ϵ of the half axes is by a factor of $(1/\epsilon)^{1/3} \cdot \sqrt{(\epsilon^2+2)/3} \geq 1$ larger than the radius of gyration of a sphere of the same volume. Thus, if one assumes that the geometric radius obtained by the fit is proportional to R_g, the radius should appear larger in the scattering experiment contrary to observation.

The dynamic behaviour of the pure microemulsion was probed with photon correlation spectroscopy. The correlation function of the scattered light intensity showed a single exponential decay at all concentrations and scattering angles. From the inverse decay times τ^{-1}, which vary linearly with the square of the momentum transfer the collective diffusion coefficient D_c was extracted as a function of the droplet volume fraction as shown in Fig. 5. By extrapolation of D_c to $\phi = 0$ a free diffusion coefficient $D_0 = 2.5 \cdot 10^{-11}\mathrm{m^2 s^{-1}}$ is obtained and the Stokes-Einstein relation yields a hydrodynamic droplet radius of $R_H = 8.5\,\mathrm{nm}$. This compares with an overall radius obtained by SAXS of $R_{SAXS} = R_\mathrm{w} + R_{AOT} = 7.1\,\mathrm{nm}$ assuming that the thickness of the AOT shell is correctly given by $R_{AOT} = 1.3\,\mathrm{nm}$ as reported in [33]. Why the hydrodynamic radius obtained by DLS is larger than the radius obtained by SAXS and also SANS [4, 34] is not entirely clear yet. However, it was suggested that the droplets are surrounded by a shell of decane molecules which adhere to the hydrophobic tails of the surfactant and thus increase the hydrodynamic radius, as the observed difference of about 1 nm compares well with the length of a decane molecule [35].

It is well known that D_c depends on the droplet volume fraction due to interparticle interactions. At low droplet volume fractions the collective diffusion constant is a linear function of ϕ [36]: $D_c(\phi) = D_0\,(1 + \lambda\phi)$ (solid line in Fig. 5) with $\lambda = -6.1$ being an interaction coefficient, which due to its sign indicates attractive interdroplet interaction. Note that up to the volume fraction of $\phi = 0.3$ $D_c(\phi)$ looks rather similar to the topologically equivalent but chemically rather different oil-in-water microemulsion with non-ionic surfactant $C_{12}E_5$ studied in [17], see inset of Fig. 5. So possibly, the flattening of $D_c(\phi)$ in the range $0.1 < \phi < 0.3$ indicates a similar crossover to an increase of D_c at higher volume fractions. Whether such an increase indicates an actual crossover to repulsive interaction at larger ϕ or whether the deviations from a linear decay are just the result of higher order terms $\mathcal{O}(\phi^2) + \ldots$ getting increasingly important remains an open question. It is also worth noting that the onset of a decreasing droplet radius (cf. Fig. 4) and the crossover in $D_c(\phi)$ both occur at about the same droplet volume fraction of $\phi \approx 0.12$. So it is likely that D_c also reflects the concentration dependence of the droplet size, which is revealed in the SAXS experiment.

B. Microemulsions with Polymers

In the following network formation upon addition of PEO-PI-PEO triblock-copolymer will be discussed in terms of structure and dynamics, the latter under both conditions of constant interdroplet distance at increasing polymer content and of constant polymer concentration at an increase of droplet volume fraction, see Fig. 1.

1. *Small Angle X-Ray Scattering*

Fig. 6 shows the SAXS intensity profiles for the microemulsion with droplet size $\omega = 40$ and a constant droplet volume fraction of $\phi = 0.1$ upon addition of increasing amounts of triblock-copolymer PEO-PI-PEO. Assuming that the size of the emulsion droplets to first approximation is unaffected by the polymer content a constant droplet volume fraction implies on average a constant interdroplet distance, which can be estimated by $d = 2R\sqrt[3]{\varrho_c/\phi}$, where d is the center to center distance, R is the droplet radius and ϱ_c is a closed packing fraction, which depends on the structure. E. g. in case of random closed packing $\varrho_c = 0.64$ a droplet radius of $R = 7.0\,\mathrm{nm}$ and a volume fraction of $\phi = 0.1$ the average distance of the polar cores is $d - 2R_\mathrm{pol} = 12\,\mathrm{nm}$, which has to be compared to an average end-to-end distance of the polyisoprene middleblock of 27 nm which we identified by light scattering. Thus, at $\phi = 0.1$ we expect a transient network to form easily.

Qualitatively, an increase in the number Z of polymer chains per droplet results in an increasing order in the system, which is reflected by the formation of a struc-

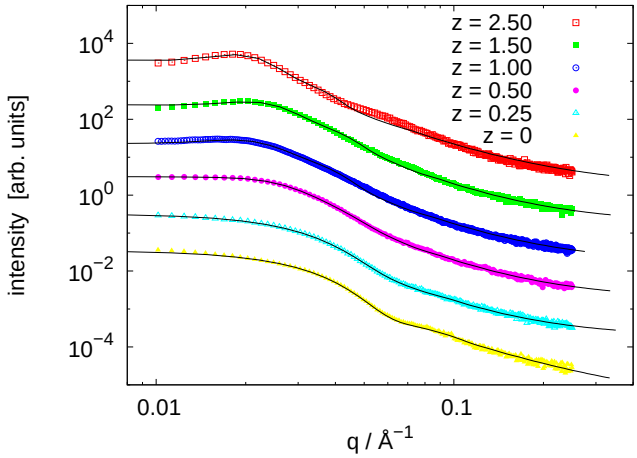

FIG. 6: (Color online) SAXS intensity profiles $I(q)$ of a microemulsion with $\omega = 40$ and $\phi = 0.1$ at increasing numbers of polymer chains per droplet Z.

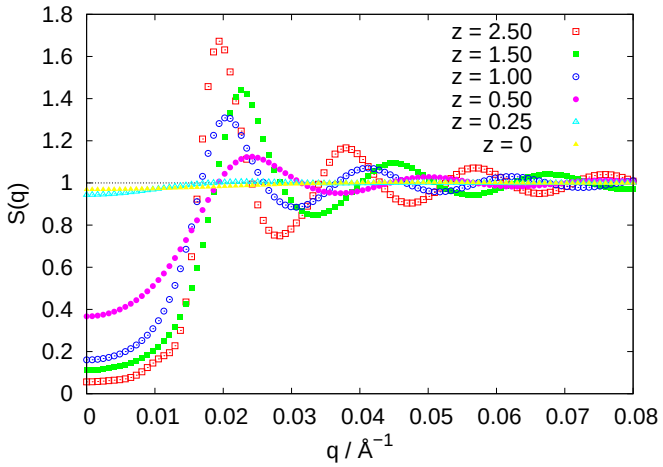

FIG. 7: (Color online) The structure factor part $S(q)$ from the fits to the SAXS intensity profiles in Fig. 6 reflects increasing order in the system with increasing polymer content.

ture peak, as can be seen in Fig. 6. The solid lines represent fits with Eq. (4). It turns out that upon addition of polymer the droplets are basically unaffected as the water core radius and also the parameter δ for the thickness of the AOT shell remain constant as a function of Z, just the radial polydispersity increases from 25% in the pure system to about 35% at $Z = 2.5$. Fig. 7 shows the structure factor part $S(q)$ of the fit functions. At lowest Z the structure factor is almost q-independent $S(q) \approx 1$ whereas around $q = 0.02\,\text{Å}^{-1}$ a structure peak emerges with growing Z. The latter fact is reflected in the hard sphere radius R_{HS} and the volume fraction of hard spheres, both of which increase continously as a function of Z. Of course the network formation is only roughly mimicked by a structure factor of hard spheres and thus the fits seen in Fig. 6 are of very good quality only at low

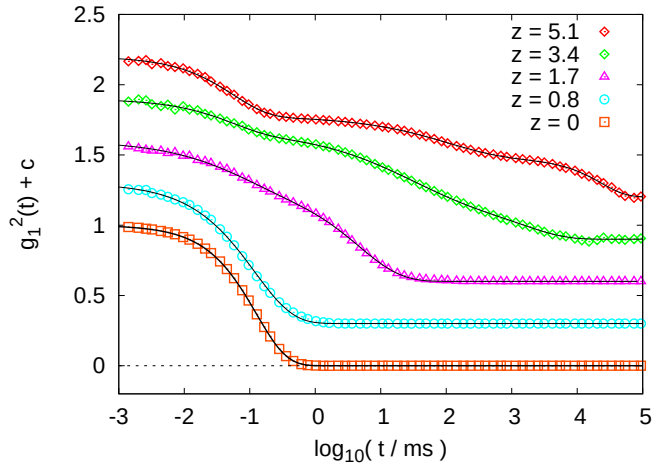

FIG. 8: (Color online) The squared electric field autocorrelation function $g_1(t)$ for a microemulsion with varying polymer content Z at $\phi = 0.1$ and $\omega = 40$ measured at $T = 298\,\text{K}$ and at a scattering angle of $2\theta = 90°$. For clarity the curves are vertically shifted. Solid lines are fits with up to three stretched exponential relaxation functions.

polymer concentrations and show noticeable deviations from the data at higher Z. These deviations are also reflected by the peak position in $S(q)$, which shows some unsystematic variation for higher Z. It should be noted that so far all attempts to improve the fit quality at larger Z by applying more elaborate models either for the structure or the form factor failed. We tried to improve the interaction potential by using the sticky-hard-sphere model suggested by Baxter [37, 38], and the form factor by considering a separate shell of polymer around the droplets and also by considering a powder average of ellipsoidal particles. However, none of the attempts brought the desired result. Whether the deviations at larger Z can be accounted for by using a recently suggested interaction potential [22], for which the Ornstein-Zernicke equation has to be solved numerically, is still an open question.

2. *Photon Correlation Spectroscopy:*

Dynamic light scattering was performed on microemulsions with triblock copolymer on the one hand as a function of polymer content at constant droplet volume fraction and on the other hand as a function of the interdroplet distance at a constant number of polymer chains per emulsion droplet Z, see Fig. 2. For the latter experiment $Z = 5.1$ was chosen and a range of volume fractions of $\phi = 0.01 \ldots 0.14$ was covered. In the former series of experiments a polymer content range of $Z = 0 \ldots 5.1$ chains per droplet at respectively constant droplet volume fractions of $\phi = 0.07$ and $\phi = 0.1$ was used. In general a slowing down of the dynamics is observed as the network forms. However, the single diffusive process, which is observed in the neat system and

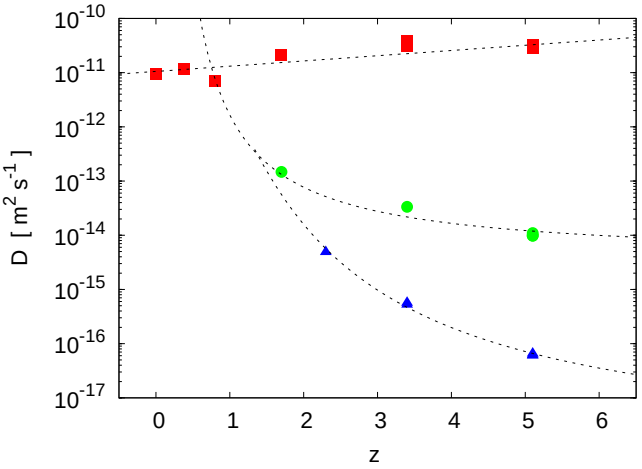

FIG. 9: (Color online) Diffusion constants of the fast (squares), intermediate (circles) and slow (triangles) relaxation process as a function of the number of polymer chains per droplet Z at constant droplet volume fraction $\phi = 0.1$. Dashed lines: guide to the eye.

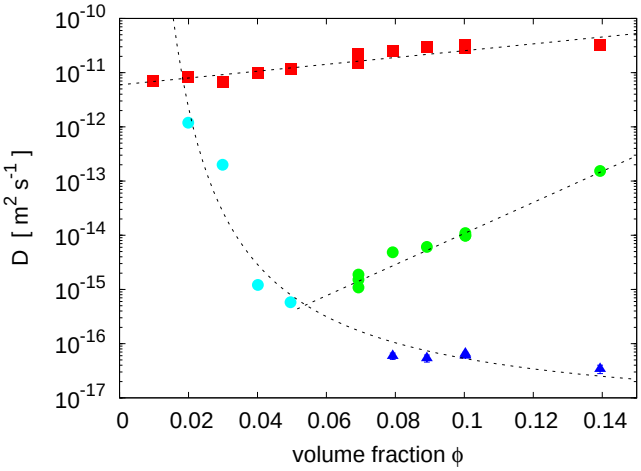

FIG. 10: (Color online) Diffusion constants of the fast (squares), intermediate (circles) and slow (triangles) relaxation process as a function of the droplet volume fraction at a constant number of polymer chains per droplet of $Z = 5.1$. Dashed lines: guide to the eye.

at very low polymer concentrations, splits up and up to three relaxation modes are observed as the network forms: Fig. 8 shows an example of the network formation as a function of polymer concentration, at a constant scattering angle of $2\theta = 90°$. The solid lines in Fig. 8 show fits with up to three stretched exponential functions $C_i(t) \propto \exp(-(t/\tau_i)^{\beta_i})$ with respective correlation time τ_i and stretching exponent β_i. Whereas for the slowest and the fastest process $\beta \approx 1$ holds in good approximation, the intermediate process turns out to be stretched at all q, where the stretching exponent varies from $\beta \approx 0.4$ at low q to $\beta \approx 0.6$ at large wave vectors. All of the observed modes reveal a diffusive wave vector dependence of the correlation times but rather differ with respect to the dependence of the apparent diffusion constants on the polymer content, as can be seen in Fig. 9. Interestingly, the fastest process accelerates and the corresponding diffusion constant increases linearly with Z as polymer is added to the system. Comparing this diffusion constant with the diffusion in the neat microemulsion the fast relaxation may be assigned to collective diffusion of the emulsion droplets in accordance with previous investigations [12]. As polymer is added the elastic forces of the polymer chains in between the droplets increase and a displaced droplet returns to its original position on a shorter timescale. The two slower processes on the other hand each slow down as polymer is added and only at the highest Z values both can be unambiguously separated.

Thus, at the value of $Z = 5.1$ network formation was studied as a function of droplet volume fraction, *i. e.* as a function of the interdroplet distance, as the SAXS results indicate that the droplet radius basically remains constant upon addition of triblock copolymer as well as upon variation of ϕ for $\phi \leq 0.14$, see Fig. 4. In Fig. 10 the results are shown: In accordance with the series of experiments shown in Fig. 9, around and above $\phi = 0.1$ three relaxation modes can be clearly distinguished. Below this volume fraction, however, only two processes and at very low ϕ just one single relaxation mode is seen. At $\phi = 0.01$ the mode is monoexponential which leads to a hydrodynamic radius of $R_H = 36\,\mathrm{nm}$. This radius may be compared with the sum of the water core droplet radius plus twice the hydrodynamic radius of the polyisoprene midblock of $R_H^{\mathrm{PI}} = 11\,\mathrm{nm}$, so $R = 6\,\mathrm{nm}{+}22\,\mathrm{nm}{=}\ 28\,\mathrm{nm}$, which is smaller than the above mentioned hydrodynamic radius of 36 nm. This finding may indicate that indeed collective diffusion of polymer decorated droplets is seen at lowest volume fractions, however with polymer loops that are somewhat stretched compared to individual free chains. This is similar to observations made in spherical block copolymer micelles, where the corona chains appear to be significantly stretched even at intermediate and low aggregation numbers [39].

As ϕ is increased the average interdroplet distance successively allows for a growing number of links in between droplets and a crossover from decorated droplets to a transient network is observed. Initially at low ϕ small aggregates form leading to a second stretched relaxation mode $0.7 \leq \beta \leq 0.85$, which is hardly distinguishable from the first relaxation at $\phi = 0.02$ but increasingly slows down and separates as the clusters grow, whereas the collective diffusion of single droplets accelerates due to the elastic properties of the polymer and stays close to a single exponential relaxation with $\beta \approx 0.9$. Around $\phi = 0.06$ the second process again splits up into a faster relaxation, which speeds up, and a slower one, which slightly slows down upon further increasing ϕ. Assuming that the second mode in the low concentration regime indeed represents cluster diffusion one might well argue that the crossover in the diffusion constants seen

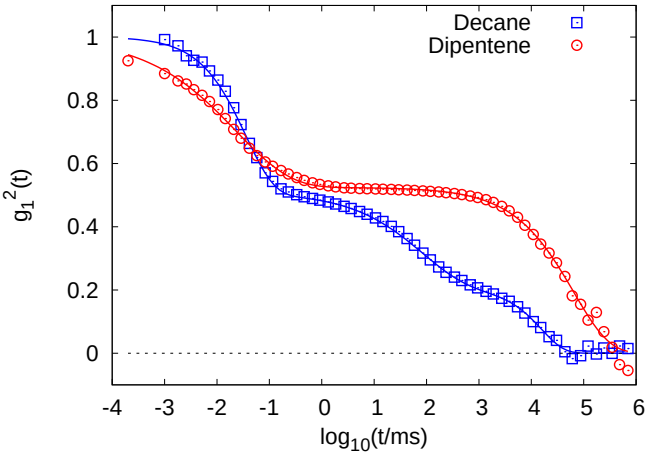

FIG. 11: (Color online) Correlation functions of a microemulsion with triblock copolymer ($Z = 5.1$ and $\phi = 0.1$) with decane and dipentene as respective continuous oil phase. Spectra were taken at $T = 298\,\mathrm{K}$ at a scattering angle of $2\theta = 130°$.

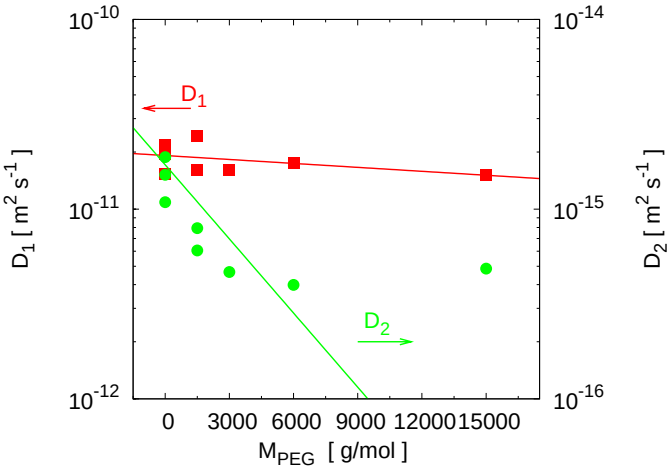

FIG. 12: (Color online) Diffusion constants of the first and the second relaxation process in a network of micelles ($\omega = 40, \phi = 0.07, Z = 5$) loaded with a mixture of water and polyethylene glycol of varying molecular weight at a concentration of $c_{\mathrm{PEO}} = 0.1\,\mathrm{g/ml}$. Multiple points at the same molecular weight represent repeated measurements of the same sample.

at $\phi \approx 0.06$ indicates percolation of the network, above which diffusion of the polymer chains and the long-range self diffusion of the droplets are possibly seen on different time scales: Whereas the droplet diffusion slows down due to the increased density of the network, polymer diffusion may speed up, as an exchange of polymer chains between droplets gets more probable at higher densities. Thus the average lifetime of a network junction point is reduced which results in an overall enhanced mobility of the polymer chains.

It should also be noted here, that similar conclusions were drawn in the literature: The slowest relaxation was interpreted in terms of self diffusion of the droplets in water-in-oil system by Stieber et al. [12] and in an inverse system by Michel et al. [21] based on light scattering and fluorescence recovery (FRAP) measurements. In a case where the intermediate relaxation appears as a diffusive process in light scattering the latter was identified with the self diffusion of the polymer chains by pulsed field gradient NMR [13]. In cases of a non-diffusive second mode it was shown for oil-in-water microemulsions [17, 18, 40] that the relaxation time was strongly correlated with the terminal relaxation time of an oscillatory shear experiment and was thus interpreted as average lifetime of the network junctions.

To further elucidate the nature in particular of the intermediate relaxation mode we performed some additional experiments: First, following an idea of Stieber et al. [25] we tried to match the refraction index of the continuous oil phase with the copolymer midblock to make the latter "invisible" for the light scattering experiment. Technically we replaced decane as the continuous oil phase with a refraction index of $n = 1.41$ [41] at ambient temperature by dipentene with a refraction index of 1.47 [42], which is closer to the refraction index $n = 1.52$ of polyisoprene [43]. The pure microemulsion with dipentene ($\omega = 40$, $\phi = 0.1$) shows one single exponential and diffusive relaxation mode, which leads to a hydrodynamic radius $R_H = 9.2\,\mathrm{nm}$ of the droplets, very close to the value of $R_H = 8.5\,\mathrm{nm}$ obtained in the decane microemulsion. Upon addition of polymer ($Z = 5.1$) only two relaxations are distinguishable. Fig. 11 shows as an example the correlation function of both microemulsions at one scattering angle: The diffusion constants associated with the slowest and the fastest mode are slightly lower in the dipentene system due to the higher viscosity of the continuous phase and, clearly, the intermediate relaxation mode vanishes upon index matching. Thus, we conclude that the latter is caused by concentration fluctuations of the polymer chains.

Of course, above a certain droplet volume fraction those concentration fluctuations should be intimately linked with the average lifetime of a network junction. In order to check this we replaced the water inside the droplets by an equal volume of an aqueous solution of polyethylene glycol (PEG) at a concentration of $c_{\mathrm{PEO}} = 0.1\,\mathrm{g/ml}$. Thus, by increasing the molecular weight of PEG the number of polymer chains contained in a droplet will decrease but at the same time the viscosity inside the droplets will increase and thus the lifetime of the network junctions is expected to rise. And indeed, at a low molecular weight of PEG ($M_{\mathrm{PEG}} = 1500\,\mathrm{g/mol}$) the observed relaxation modes coincide with those found in a water core microemulsion at comparable Z. Upon increasing M_{PEG}, however, the second relaxation mode is significantly slowed down, whereas the first mode basically remains unchanged, as is demonstrated in Fig. 12. Thus, the dynamics of the triblock and the lifetime of network junctions is influenced as expected, which corroborates

the above made assignment of the second relaxation with concentration fluctuations of the interconnecting polymer chains.

V. CONCLUSIONS

We observe network formation upon addition of PEO-PI-PEO triblock copolymer to a water-AOT-decane microemulsion. Of course up to that point it cannot be entirely excluded from an experimental point of view that the triblock copolymer forms micelles of its own in the continuous oil phase, as such polymer micelles would also lead to an increasing structural order and a slowing down of the dynamics in the system. However, there are several points that indicate that indeed the hydrophilic ends of the polymer stick into the droplets: First, we added simple PI of the same molecular weight as the midblock of the copolymer to a pure microemulsion ($\omega = 40, \phi = 0.1$) at a concentration that corresponds to a concentration of PI for $Z = 5$ triblock chains per droplet and observed depletion induced phase separation into a polymer-rich and a dense droplet phase, which is well known in colloidal systems [44]. If PEO-PI-PEO formed its own micelles one would expect similar effects on the stability of the microemulsion as those obtained by adding pure PI, which is not observed. Thus, the PEO ends stick into the water droplets and by that even stabilise the microemulsion, which is seen by the fact that at $Z = 5$ additional polymer PEG of intermediate and even large molecular weight may be loaded into the droplets without destroying the microemulsion structure in contrast to an emulsion with $Z = 0$, which only was stable for the lowest molecular weight of $M_{\mathrm{PEG}} = 1500\,\mathrm{g/mol}$.

What is also hard to determine, in general, is whether the triblock copolymer just decorates single droplets or actually forms bridges in between droplets. In particular our measurements at constant Z and varying interdroplet distance indicate that there is indeed diffusion of decorated droplets at very low ϕ and then, as the droplet volume fraction increases, a diffusion of clusters up to the point of percolation. In fact it was shown in molecular dynamics simulation studies that the dynamics of the transient network is basically determined by the ratio of decorating vs. bridging polymer chains ("link-to-loop ratio") [45]. And recent theoretical work even predicted that the competition between decorating and bridging polymers leads to an entropy driven first order phase transition from a liquid droplet phase to a highly connected network in equilibrium with a dilute solution of decorated droplets [46]. Although we clearly did not observe the latter in our systems it may still be that the polymer concentration was too low, and that at higher Z a crossover into a two-phase system would be observable.

When comparing our results with the behaviour of polymer induced networks in direct oil-in-water microemulsions [17, 20, 21] it turns out that with respect to structure and dynamics on the first sight both are rather similar: Even in the pure microemulsion system topology seems to govern the behaviour, as a similar crossover is observed in the concentration dependence of the collective diffusion constant. In detail, however, dynamics shows different behaviour: Whereas in our system, in accordance with previous findings, up to three diffusive relaxation modes were distinguishable by light scattering, in comparable o/w systems either a non-diffusive mode [17] or a crossover from diffusive to non-diffusive behaviour was observed [20, 21]. Such kind of behaviour was recently analysed by Michel *et al.* in terms of the generalised Brochard-de Gennes Two-Fluids-Model [47]. As the model describes the dynamics of a viscoelastic system characterised by a terminal relaxation time τ_R and an instantaneous elastic modulus G_0 it produces at most two different monoexponential relaxations. Michel *et al.* applied the model on the fastest two relaxation modes in their system [21], but in general the assignment is not *a priori* evident in case of more than two relaxations. Moreover, in our system, as there are no systematic deviations from diffusive behaviour of the relaxation modes, any further hints are missing as to which mode the model should be applied for. Thus, we refrained from considering it any further.

Concluding, it has become clear that indeed the hydrophilic ends of the triblock copolymer chains stick inside the water droplets to form decorating loops at lowest droplet volume fractions and crosslinks in between droplets as the volume fraction increases. As the network forms the increasing order in the system is reflected in a pronounced structure factor, which only at low to intermediate polymer content can sufficiently be modelled by a structure factor of hard spheres. In the dynamics apart from collective droplet diffusion on short timescales and long-range self diffusion of droplets and/or clusters at long times, above the percolation transition an additional intermediate mode is seen, which is related to concentration fluctuations of the polymer chains, as it vanishes upon index matching of the continuous oil phase with the midblock and slows down upon loading the droplets with long-chain polymers. Whether such behaviour can finally be understood in the framework of a viscoelastic model similar to the one mentioned above that reproduces all three relaxation modes has to be left open for further work.

[1] M. S. Green and A. V. Tobolsky, J. Chem. Phys. **14**, 80 (1946).

[2] S. K. Kumar and A. Z. Panagiotopoulos, Phys. Rev. Lett. **82**, 5060 (1999).

[3] A. G. Zilman and S. A. Safran, Phys. Rev. E **66**, 051107 (2002).

[4] M. Kotlarchyk, S.-H. Chen, J. S. Huang, and M. W. Kim, Phys. Rev. A **29**, 2054 (1984).

[5] R. Pecora, ed., *Dynamic Light Scattering — Applications of Photon Correlation Spectroscopy* (Plenum, New York, 1985).

[6] W. Brown, ed., *Dynamic Light Scattering: The Method and Some Applications* (Clarendon, Oxford, 1993).

[7] P. N. Pusey and W. van Megen, Physica A **157**, 705 (1989).

[8] J. G. H. Joosten, E. T. F. Geladé, and P. N. Pusey, Phys. Rev. A **42**, 2161 (1990).

[9] C. Quellet, H.-F. Eicke, G. Xu, and Y. Hauger, Macromolecules **23**, 3347 (1990).

[10] H.-F. Eicke, U. Hofmeier, C. Quellet, and U. Zölzer, Progr. Colloid Polym. Sci. **90**, 165 (1992).

[11] M. Odenwald, H.-F. Eicke, and W. Meier, Macromolecules **28**, 5069 (1995).

[12] F. Stieber, U. Hofmeier, H.-F. Eicke, and G. Fleischer, Ber. Bunsenges. Phys. Chem. **97**, 812 (1993).

[13] G. Fleischer, F. Stieber, U. Hofmeier, and H.-F. Eicke, Langmiur **10**, 1780 (1994).

[14] R. Hilfiker, H.-F. Eicke, C. Steeb, and U. Hofmeier, J. Phys. Chem. **95**, 1478 (1991).

[15] H.-F. Eicke, C. Quellet, and G. Xu, Colloids Surf. **36**, 97 (1989).

[16] H. Bagger-Jörgensen, L. Coppola, K. Thuresson, U. Olsson, and K. Mortensen, Langmiur **13**, 4204 (1997).

[17] M. Schwab and B. Stühn, J. Chem. Phys. **112**, 6461 (2000).

[18] E. Michel, M. Filali, R. Aznar, G. Porte, and J. Appell, Langmuir **16**, 8702–8711 (2000).

[19] M. Filali, M. J. Ouazzani, E. Michel, R. Aznar, G. Porte, and J. Appell, J. Phys. Chem. B **105**, 10528 (2001).

[20] E. Michel, L. Cipelletti, E. d'Humieres, Y. Gambin, W. Urbach, G. Porte, and J. Appell, Phys. Rev. E **66**, 031402 (2002).

[21] E. Michel, G. Porte, L. Cipelletti, and J. Appell, Langmuir **20**, 984 (2004).

[22] G. Porte, C. Ligoure, J. Appell, and R. Aznar, J. Stat. Mech. p. P05005 (2006).

[23] S. R. Bhatia, W. B. Russel, and J. Lal, J. Appl. Cryst. **33**, 614 (2000).

[24] I. Lynch and L. Piculell, J. Phys. Chem. B **108**, 7515–7522 (2004).

[25] F. Stieber and H.-F. Eicke, Colloid Polym. Sci. **274**, 826–835 (1996).

[26] S. Chen, J. Rouch, F. Sciortino, and P. Tartaglia, J. Phys.: Condens. Matter **6**, 10855 (1994).

[27] U. Batra, W. B. Russel, M. Pitsikalis, S. Sioula, J. W. Mays, and J. S. Huang, Macromolecules **30**, 6120 (1997).

[28] J. B. Hayter, in *Physics of Amphiphiles: Micelles, Vesicles and Microemulsions*, edited by V. Degiorgio and M. Corti (Elsevier, Amsterdam, 1985), pp. 59–93.

[29] M. Schwab and B. Stühn, Colloid Polym. Sci. **275**, 341 (1997).

[30] M. S. Wertheim, Phys. Rev. Lett. **10**, 321 (1963).

[31] E. Thiele, J. Chem. Phys. **39**, 474 (1963).

[32] H. Seto, M. Nagao, Y. Kawabata, and T. Takeda, J. Chem. Phys. **115**, 9496–9502 (2001).

[33] S. H. Chen, Ann. Rev. Phys. Chem. **37**, 351–399 (1986).

[34] M. Kotlarchyk, S.-H. Chen, and J. S. Huang, J. Phys. Chem. **86**, 3273 (1982).

[35] M. W. Kim, W. D. Dozier, and R. Klein, J. Chem. Phys. **84**, 5919–5921 (1986).

[36] P. N. Pusey and R. J. A. Tough, in *Dynamic Light Scattering: Applications of Photon Correlation Spectroscopy*, edited by R. Pecora (Plenum Press, New York, London, 1985), chap. 4, p. 85–179.

[37] R. Baxter, J. Chem. Phys. **49**, 2270 (1968).

[38] R. Baxter, J. Chem. Phys. **52**, 4559 (1970).

[39] S. Förster, E. Wenz, and P. Lindner, Phys. Rev. Lett. **77**, 95–98 (1996).

[40] U. Zölzer and H.-F. Eicke, J. Phys. II France **2**, 2207 (1992).

[41] J. A. Riddick and W. B. Bunger, *Organic Solvents* (Wiley-Interscience, New York, 1970).

[42] D. R. Lide, ed., *CRC Handbook of Chemistry and Physics* (CRC Press, New York, 1997).

[43] J. Brandrup, E. H. Immergut, and E. A. Grulke, eds., *Polymer Handbook* (Wiley, New York, 1999).

[44] W. C. K. Poon, J. Phys.: Condens. Matter **14**, R859–R880 (2002).

[45] T. Koga and F. Tanaka, Eur. Phys. J. E **17**, 115–118 (2005).

[46] A. Zilman, J. Kieffer, F. Molino, G. Porte, and S. A. Safran, Phys. Rev. Lett. **91**, 015901 (2003).

[47] F. Brochard and P. G. de Gennes, Macromolecules **10**, 1157–1161 (1977).